TITLE: LIKELIHOOD OF SAMPLING PROSTATE CANCER AT SYSTEMATIC BIOPSY AS A FUNCTION OF GLAND VOLUME AND NUMBER OF CORES

RUNNING TITLE: PROSTATE SIZE IMPACTS THE ABILITY TO SAMPLE CANCER AT BIOPSY

Michael E. Rezaee[1], Katarzyna J. Macura[2], Bruce J. Trock[1,3], Amin Herati[1], Christian P. Pavlovich[1], Misop Han[1], Dan Stoianovici[1]

[1]The James Buchanan Brady Urological Institute and Department of Urology, [2]Department of Radiology, [3]Bloomberg School of Public Health

Johns Hopkins University School of Medicine, Baltimore, Maryland, USA

Corresponding Author: Dan Stoianovici, PhD, Robotics Laboratory, Department of Urology, Johns Hopkins University School of Medicine, 5200 Eastern Ave, Baltimore, MD 21224, Tel: (410) 550-1980, E-mail: dss@jhu.edu

Keywords: Prostate Biopsy, Prostate Cancer, TRUS, Biopsy plan, MRI

ABSTRACT

BACKGROUND: Pre-biopsy multiparametric magnetic resonance imaging (mpMRI) of the prostate is used to conduct targeted prostate biopsy (TB), guided by ultrasound and registered (fused) to the MRI. Systematic biopsy (SB) continues to be used together with TB or in mpMRI negative patients. There is insufficient evidence on how to use SB to inform clinical decision-making in the mpMRI era. The purpose of this study was to estimate the effect of prostate volume and number of SB cores on sampling clinically significant prostate cancer (csPCa) using a simulation method using clinical data.

METHODS: SBs were simulated using data from 42 patients enrolled in a transrectal ultrasound robot-assisted biopsy trial. Linear mixed models were used to examine the relationship between the number of SB cores and prostate volume on 1) clinically significant cancer detection probability (csCDP) and 2) percent of mpMRI depicted regions of interest (ROIs) sampled with the SB.

RESULTS: Median values and interquartile range (IQR) were 47.16 cm^3 (35.61-65.57) for prostate volume, 0.57 cm^3 (0.39 - 0.83) for ROI volume, and 4.0 (2 - 4) for PI-RADS v2.1 scores on MRI. csCDP increased with the increasing number of simulated SB cores and decreased substantially with larger prostate volume. Similarly, the percent of ROIs sampled increased with the increasing number of simulated SB cores and was lower for prostate volumes $\geq$60 cm^3 compared to glands < 60 cm^3.

CONCLUSIONS: The effect of the number of SBs performed on detecting csPCa varies largely with gland volume. The common 12-core SB can achieve adequate cancer detection and sampling of ROIs in smaller glands, but not in larger glands. In addition to TB or in mpMRI negative patients, the number of SB cores can be adjusted to prostate volume. Performing 12-core SB alone in $\geq$60 cm^3 glands results in inadequate sampling and potential PCa underdiagnosis.

INTRODUCTION

In the era of pre-biopsy multiparametric magnetic resonance imaging (mpMRI) of the prostate, systematic biopsy (SB) can detect clinically significant prostate cancer (csPCa) that is not detected by MRI-targeted biopsy (TB) alone in up to 22% of patients [1-5] [6]. SB alone typically is used for men with negative mpMRI [4]. However, the concept of SB is somewhat of a fallacy. Significant discrepancy exists between planned SBs and the location of actual cores obtained [7]. Urologists are known to biopsy in clustered patterns and undersample large portions of the gland [7], especially the anterior and apical regions of the prostate [8, 9]. Moreover, SBs commonly use the same 12-core extended sextant plan for all patients [10]. Reducing the number of SB cores when used in conjunction with TB [10] or eliminating SB all together in mpMRI negative patients [11] are also considered. Thus, current SB is more of a variable sampling strategy than is typically appreciated [12].

SB techniques have improved over the years to increase csPCa detection probability (csCDP). The most notable changes have been to 1) increase in the number of cores (6 to 12) as well as lateral displacement of these additional cores [13]; 2) employing a uniform grid-based approach to reduce urologist sampling error [12]; and 3) account for gland anatomy and the location of potential regions of interest (ROIs) within the gland to maximize csCDP [14].

We have also developed a novel, systematic biopsy optimization methodology [15, 16] that considers the anatomy of the prostate gland, urethra, ROIs on mpMRI, and best approach angle of the biopsy needle to optimize csCDP [17], and so defines a personalized biopsy plan for each patient. In this study we employ personalized biopsy planning methods to investigate the influence of the number of cores and prostate volume on cancer sampling outcomes.

MATERIALS and METHODS

Systematic Biopsy Plan Optimization

SB plans with an increasing number of cores were simulated on images from 42 consecutive patients that were randomized to the robot arm of our robot-assisted versus UroNav (Philips Corp.) biopsy trial (NCT02871726) [18]. The study was approved by the Johns Hopkins Institutional Review Board #00068488. Patients enrolled in the trial were ages 45 to 75, had an indication for prostate biopsy, and underwent pre-biopsy mpMRI. Patient characteristics are shown in Table 1. Continuous variables are compared with Mann-Whitney test, and categorical variables are compared with chi-squared. As shown, there were no significant differences between the Robot and UroNav patient characteristics, and representative of the prostate biopsy patient population. All mpMRI were interpreted according to PI-RADS v2.1 [19] by a single radiologist (KM) specialized in PCa. The aims of the simulation were to evaluate the joint influence of the number of SB cores and prostate volume on the 1) csCDP and 2) percentage of ROIs successfully sampled by SB alone.

Table 1: Patient characteristics, Median (IQR)

Variable	Robot Arm	UroNav Arm	P-Value
Age	65 (60-69)	65 (57.3-69)	0.50
PSA [ng/ml]	6 (4.2-9.9)	6.3 (4.5-8.1)	0.97
Prostate volume [cm^3]	47.2 (35.6-65.6)	54.0 (32.4-74.7)	0.92
PSA Density [$ng/ml/cm^3$]	0.13(0.09-0.18)	0.12(0.09-0.21)	0.86
PI-RADS v2.1 [1-5]	4 (2-4)	4 (2-4)	0.35
PI-RADS < 3	33%	29%	0.7
Number of ROI > 1	33%	26%	0.49
Previous biopsy > 0	45%	32%	0.27

An example with a 12-core SB plan optimized for one of the patients is shown in Figure 1. A capsule is centered on a core and has a cylindrical shape with spherical ends. Its radius is ~5mm, equaling that of the smallest spherical csPCa ($0.5cm^3$ [20]). Any part of a csPCa lesion present within the capsule is therefore equivalent to its core sampling the lesion [15]. As such, the degree with which the capsules fill the gland may be used to quantify csCDP. Please see the Supplement for additional information.

Figure 1a shows the capsules filling the volume of the gland. Figure 1b shows the cores of the same biopsy plan. The plan was generated without knowledge of the ROIs. Even so, the image shows that 2 of the 3 ROIs were intersected by cores, in this example.

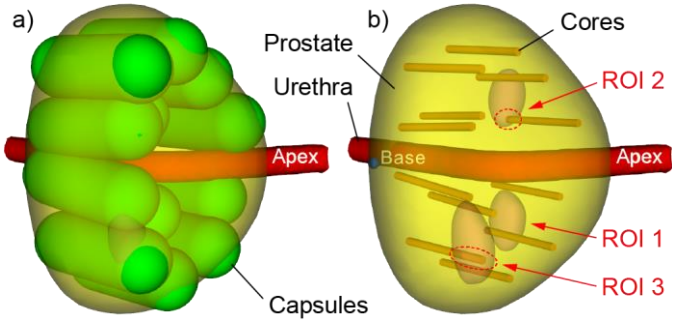

Figure 1: SB plan for one of the patients: Prostate volume 41cm^3, three ROI, 12-core personalized SB plan: a) Prostate filled with Capsules resulting in 51% csCDP; b) The same SB plan showing biopsy core distribution and how 2 of the 3 MRI ROI were sampled. Dotted red ovals show where the core intersected the ROI: ROI1 was not sampled, ROI2 was sampled by 1 core over 1.35mm, and ROI3 by 1 core over 4.15mm. The other cores did not cross ROIs.

Statistical Analysis

Descriptive statistics were used to summarize patient data. Because there were 24 simulated biopsies (with varying core numbers from 1 to 24) for each patient, a linear mixed model was used to examine the association between the number of SB cores and prostate volume on csCDP. For this model, prostate volume was treated as continuous and random coefficients were used (i.e. both the intercept and number of biopsy cores were treated as random effects).

A similar linear mixed model was used to examine the association between the number of SB cores and prostate volume on the percentage of ROIs successfully sampled by simulated biopsies. For this model, prostate volume was dichotomized at 60 cm^3 for Aim 2. A ROI was considered to be "sampled" if it was intersected by at least one biopsy; thus each ROI was considered to be sampled or unsampled. For each number of cores 1 to 24, for all prostates within the group (smaller and larger than 60 cm^3) the software defined a biopsy plan and counted the number of ROIs sampled. The ROI sampling rate was defined as the total number of sampled lesions to the total number of lesions within the group. All models were evaluated based on the Wald test for each variable in the model, and comparison of Akaike's Information Criterion (AIC) as each additional variable is added to the model.

RESULTS

Data from 42 patients was used to simulate biopsies with 1 to 24 cores each, resulting in 1008 experiments. Median values and interquartile range (IQR) were 47.16 cm^3 (35.61-65.57) for prostate volume, 0.57 cm^3 (0.39 - 0.83) for ROI volume, and 4.0 (2 - 4) for PI-RADS v2.1 scores.

csCDP as a Function of the Number of Cores and Prostate Volume

Figure 2 displays the relationship between csCDP and the number of SB cores and prostate volume.

Using our biopsy optimization methodology, csCDP improved with the increasing number of SB cores (β = 4.11, p<0.0001) and decreased with increasing prostate volume (-0.201, p<0.0001). Adding the interaction term improved model fit compared to the model with only main effects, indicated by the smaller (better) AIC, 5984.4 vs. 6011.4, and the statistically significant interaction coefficient. The negative value for the interaction coefficient in the linear mixed model (β = -0.023, p<0.001) indicates that, for a fixed prostate volume, once a large fraction of the prostate volume is sampled, subsequent increases in the number of SB cores bring diminishing increases in csCDP (Table 2).

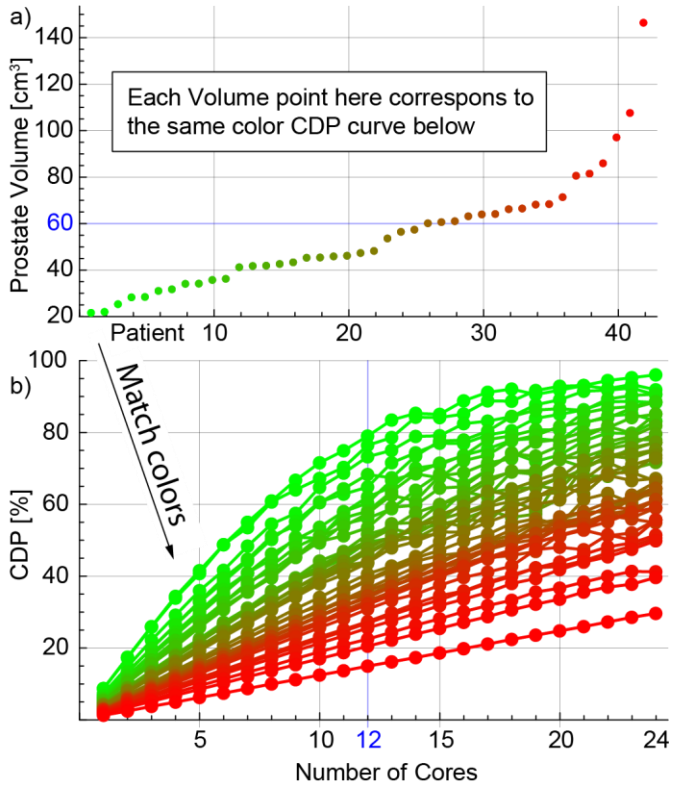

Figure 2: a) Sorted prostate volumes of the patients and b) csCDP vs. number of cores for each volume.

Thus, for smaller prostate glands, a certain number of SB cores will sufficiently sample most of the prostate volume. Increasing the number of SB cores did not result in a linear increase in csCDP for smaller glands. For example, in the smallest gland (20.99 cm^3), csCDP was 80% for a standard 12-core SB and 95% for a 24-core SB biopsy; only a 15% increase in csCDP was obtained when doubling the number of SB cores. Alternatively, in the largest prostate gland (145.77 cm^3), csCDP was 20% for a standard 12-core SB biopsy and 40% for a 24-core SB biopsy. A 20 percentage point increase in csCDP was achieved when doubling the number of SB cores in the largest gland, but most of the gland still remained unsampled (60%).

Table 2: Linear mixed model of association between CDP vs. number of SB cores and prostate volume

Variable	**Estimated Coefficient**	**P-Value**
Intercept	17.68	-
Number of biopsy cores	4.11	<0.0001
Prostate volume (cm^3)	-0.201	<0.0001
Number of cores x Prostate volume	-0.023	<0.0001
AIC for interaction vs. main effects model	5984.4 vs. 6011.4	-

ROI Sampling Rate as a Function of the Number of Cores and Prostate Volume

Figure 3 displays the relationship between percent of ROIs sampled, the number of SB cores, and prostate volume.

The relationship between percent of ROIs sampled and SB cores differed between prostate glands <60 (26 patients) versus those >=60 cm^3 (15 patients; one patient had no ROIs identified). Similar to csCDP analyses above, the percent of ROIs sampled increased with the number of SB cores and was smaller for prostate volume $\geq$60 cm^3 than for glands < 60 cm^3 (Table 3).

The slope of percent of ROIs sampled begins to plateau with an increasing number of SB cores for smaller glands. Almost 70% of ROIs were sampled via a standard 12-core SB. Increasing the number of SB cores to 24 resulted in just under 90% of ROIs being sampled; only 20% increase by doubling the number of cores.

The percentage of ROIs sampled was lower for large glands >=60 cm^3. In these cases, the slope of the percent of ROIs sampled holds its gradient steadier with an increasing number of cores (Figure 3). Even at a max of 24 SB cores only 65% of ROIs are sampled, while only 45% of ROIs are sampled in a standard 12-core SB.

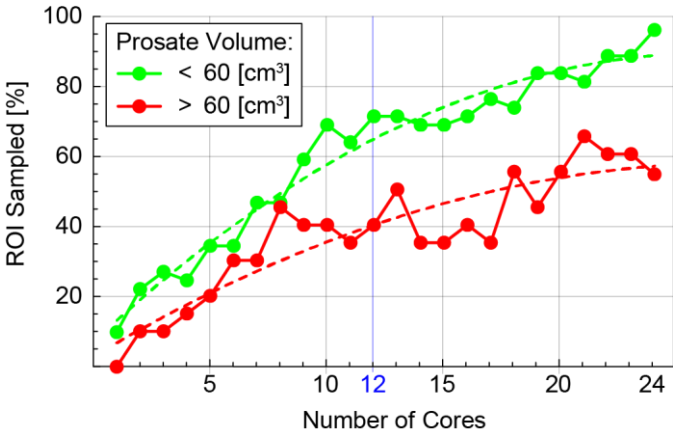

Figure 3: ROI Sampling Rate versus the Number of SB Cores for Prostate Volumes within two groups < 60 cm^3 and > 60 cm^3). Dotted curves show a quadratic fit.

Table 3: Linear mixed model of percent of ROIs sampled by biopsy vs. number of SB cores, prostate volume, highest ROI PI-RADS v2.1 score, and highest ROI volume.

Variable	**Estimated Coefficient**	**P-Value**
Intercept	0.052	-
Number of biopsy cores	0.036	<0.0001
Prostate volume (cm^3)	-0.113	0.184
Number of cores x Prostate volume	-0.014	0.003
ROI PI-RADS v2.1 score	-0.005	0.833
ROI volume (cm^3)	0.238	<0.0001
AIC for interaction vs. main effects model	590.1 vs. 596.2	-

DISCUSSION

A SB simulation study was performed using clinical trial data. It showed that the effect of the number of cores on the likelihood of sampling csPCa depends largely on the gland volume. Sampling csPCa in larger prostates is substantially more challenging.

The concept of increasing CDP by increasing the number of prostate biopsies has previously been described as linearly dependent [21, 22]. However, our simulation reveals that this relationship is overall nonlinear, except for the first cores. In our model, to increase CDP a biopsy plan must fill the gland with capsules as much as possible. Each one of the initial cores contributes equally to CDP because there is sufficient room within the gland to fully fit each additional capsule. Observe how all graphs in Figure 2b are linear for a low number of cores, and how the linear part is shorter for smaller glands (green) compared to larger ones (red). Depending on the gland volume, after the first several cores, the capsules start to overlap and so their individual contribution to csCDP gain

becomes progressively lower. This can be seen in Figure 2b as the csCDP curves begin to plateau with increasing number of cores, while occurring earlier for smaller glands. For example, for the smallest gland (20.99 cm^3) in the study, csCDP was nearly 80% for a standard 12-core SB and 95% for a 24-core SB plan; only a 15-percentage point increase in csCDP was achieved when doubling the number of SB cores. This plateau in CDP with additional SB cores was also observed by Kanao et al. in their simulation of different biopsy depths and cutting lengths [14]. In contrast, the csCDP curves for larger glands are much longer linear (red curves) indicating that additional cores are more important in larger glands. For example, for the largest gland (red) in Figure 2b the entire curve is linear because there is sufficient room within the gland to fully fit all 24 capsules. Lee et al., also in a simulation study, indicated that at least 1 SB core is needed for every $2cm^3$ of prostate volume (23 cores in $43.5cm^3$) [10], which in our study corresponds to approximately 80% CDP.

Performing a greater number of biopsies in larger glands to increase csCDP raises safety concerns [23, 24]. Moreover, several studies have failed to demonstrate improved csCDP when increasing the number of SBs performed [25]. For example, De La Taille et al. did not find a significant difference in CDP between a sextant (22.7%), 12-core (28.3%), 18-core (30.7%), and 21-core biopsy plan [26]. Based on our simulation, saturation biopsies may not actually saturate. As can be seen in Figure 3, the csCDP in the largest gland ($145.77cm^3$) in the simulation was 15% for a 12-core and 30% for a 24-core biopsy leaving 70% of the gland unsampled. Assuming a continued linear slope in csCDP, 64 cores would be needed to obtain a csCDP of 80%. Currently, the utility of extended core or "saturation" biopsy is considered to be low and they are no longer routinely used in practice [27].

In the era of mpMRI of the prostate, CDP may not be as important a measure compared to understanding the percent of ROIs that are sampled by SB. As seen in Figure 3, nearly 70 and 90% of ROIs were sampled in glands <60 cm^3 (green line) with a 12 and 24-core SB, respectively. Thus, most ROIs can be sampled on SB alone when glands are small. However, when glands are large (>=60 cm^3, Figure 3 red line), only 40% and 55% of ROIs are sampled with a 12 and 24-core SB, respectively. Thus, the clinical utility of SB is highly dependent on gland size with larger glands likely requiring additional cores to sample a greater number of ROIs. This highlights the importance of TB especially for large glands and likely partially explains why SB alone with the common 12-core extended sextant biopsy plan has historically performed poorly compared to modern biopsy approaches [1].

Although it is reasonable to obtain an mpMRI of the prostate prior to biopsy, the AUA currently does not regard such imaging as standard of care [4]. However, our simulation suggests that the role of TB is critical especially in men with larger glands who are severely under-sampled with a 12-core standard SB. In contrast, men with small glands may be adequately sampled with SB in the absence of MRI. However, MRI is the primary method of estimating the size of the prostate prior to biopsy, and so omitting an MRI is problematic. Nevertheless, a biopsy without a fusion system can be considered in a small gland.

Furthermore, with almost 60% of urologists who perform biopsies reporting the same or increased use of TRUS SB without MRI in 2022 [28], we must recognize that a substantial proportion of patients with large glands are likely insufficiently sampled with SB alone. Thus, pre-biopsy mpMRI of the prostate to potentially target suspicious lesions may be particularly beneficial in patients with large prostate glands. However, barriers exist to obtaining a high-quality pre-biopsy mpMRI of the prostate in every patient with indication for prostate biopsy in the U.S. [29]. Alternatively, pre-biopsy ultrasound may be used to measure the gland, and depending on size to make an informed decision about obtaining an MRI.

The current practice of performing TB and SB combined improves overall cancer detection but also requires an increased number of cores and potentially resultant patient morbidity. To reduce the number of cores, a retrospective analysis on 971 biopsies found that discarding SB cores that were distal from TB ROIs caused a very small loss of sampled cancer (at 2 cm from target with 3.8 fewer cores combined CDP dropped from 44.8% to 44%) [30]. This finding supports the importance of MRI for biopsy targeting, but prostate volume was not yet considered.

For patients without significant mpMRI findings (PI-RADS < 3) studies have carefully recommended SB due to concerns related to the sensitivity of MRI and expertise in interpretation [31]. But approximately one-third of men

who have an indication for prostate biopsy have negative mpMRI findings, going up to 50% in expert centers, and so skipping SB in this population could potentially avoid numerous biopsies [11]. Ideally, with improved MRI and TB targeting the number of biopsies would be reduced to 1 or none. However, with current methods and devices TB alone does not necessarily result in accurate sampling due to mpMRI, fusion, and needle targeting errors and so additional SB cores are normally taken. Our study suggests that the number of SB cores should be adjusted to the prostate volume with varying number of cores and considering the number and location of TB cores. In large glands, however, safety concerns will limit the number of cores and the ability to adequately sample the gland at SB, thus underscoring the importance of TB and accurate targeting.

Performing an adequate prostate biopsy is uniquely challenging compared to sampling other organs. Tumors within the gland are typically small, may or may not be seen on imaging, and may be difficult to access depending on biopsy approach. There is also substantial variation and sampling error introduced by urologists performing biopsies [7]. To address these challenges 3D renderings of the gland with new sampling strategies have been proposed. For example, Ahmed et al. recently described a grid-based schema that utilizes detection squares to guide comprehensive sampling of the prostate gland [12]. Similarly, Kanao et al. demonstrated improved CDP with altering biopsy cutting length and depth based on 3D volume and zonal anatomy [14]. Unlike these approaches, our biopsy optimization accounts for anatomy of the prostate gland, urethra, ROIs, and best approach angle of the biopsy needle to sample tissue. Determination of the best approach to SB and its continued role independent of or in addition to TB will rely on future comparative studies.

There are limitations of our study to consider. First, this is an image processing simulation study. Thus, our biopsy results reflect a truer systematic plan of sampling the prostate compared to what is currently carried out in clinical practice with SB. However, csCDP and the percent of ROIs sampled may be lower based on "freehand" SB data given the known sampling error of urologists [7]. Moreover, simulation results consider a perfectly executed biopsy plan, and so practical results would also be lower. Lastly, we focused on prostate volume but did not account for ROI volume. ROI volume in MRI clearly impacts sampling of csPCa at biopsy and resulting pathology [32]. But our study explored the SB alone and so the algorithms were blinded to the location of ROIs and their volume.

Our simulation is based on data from transrectal biopsies [33], however the methodology applies to transperineal biopsy as well [15]. The csCDP and ROI sampling numbers would slightly change with the different orientation of the needles, but we believe that the general relationship with the number of cores and prostate volume holds.

CONCLUSION

Our simulation analysis of a novel biopsy optimization methodology indicates that the effect of the number of SBs performed on detecting csPCa varies with gland volume. SB may achieve adequate cancer detection and sampling of ROIs in small glands even without pre-biopsy mpMRI and TB, but not in larger glands where TB are likely needed to maximize detection while maintaining a low number of cores. Not using TB on large prostates is likely to result in inappropriate sampling.

ACKNOWLEDGEMENTS

Research reported in this publication was supported by the National Cancer Institute of the National Institutes of Health under Award Number R01CA247959.

DISCLOSURE

Under a license agreement between Eigen Health Services and the Johns Hopkins University, author DS and the University are entitled to royalty distributions related to technology described in this article. This arrangement has been reviewed and approved by the JHU in accordance with its conflict-of-interest policies.

REFERENCES

1. Kasivisvanathan V, Rannikko AS, Borghi M, Panebianco V, Mynderse LA, Vaarala MH, Briganti A, Budaus L, Hellawell G, Hindley RG, Roobol MJ, Eggener S, Ghei M, Villers A, Bladou F, Villeirs GM, Virdi J, Boxler S, Robert G, Singh PB, Venderink W, Hadaschik BA, Ruffion A, Hu JC, Margolis D, Crouzet S, Klotz L, Taneja SS, Pinto P, Gill I, Allen C, Giganti F, Freeman A, Morris S, Punwani S, Williams NR, Brew-Graves C, Deeks J, Takwoingi Y, Emberton M, Moore CM, Collaborators PSG: MRI-Targeted or Standard Biopsy for Prostate-Cancer Diagnosis. *N Engl J Med.* May 10 2018; Vol.378(19) pp.1767-1777. https://www.ncbi.nlm.nih.gov/pubmed/29552975. PMCID:29552975
2. Padhani AR, Barentsz J, Villeirs G, Rosenkrantz AB, Margolis DJ, Turkbey B, Thoeny HC, Cornud F, Haider MA, Macura KJ, Tempany CM, Verma S, Weinreb JC: PI-RADS Steering Committee: The PI-RADS Multiparametric MRI and MRI-directed Biopsy Pathway. *Radiology.* Aug 2019; Vol.292(2) pp.464-474. https://www.ncbi.nlm.nih.gov/pubmed/31184561. PMCID:31184561
3. Romero D: Targeted biopsy reduces detection of clinically insignificant cancer. *Nat Rev Clin Oncol.* Feb 2023; Vol.20(2) pp.63. https://www.ncbi.nlm.nih.gov/pubmed/36600007. PMCID:36600007
4. Wei JT, Barocas D, Carlsson S, Coakley F, Eggener S, Etzioni R, Fine SW, Han M, Kim SK, Kirkby E, Konety BR, Miner M, Moses K, Nissenberg MG, Pinto PA, Salami SS, Souter L, Thompson IM, Lin DW: Early Detection of Prostate Cancer: AUA/SUO Guideline Part II: Considerations for a Prostate Biopsy. *J Urol.* Apr 25 2023; pp.101097ju0000000000003492. PMCID:37096575
5. Ahdoot M, Wilbur AR, Reese SE, Lebastchi AH, Mehralivand S, Gomella PT, Bloom J, Gurram S, Siddiqui M, Pinsky P, Parnes H, Linehan WM, Merino M, Choyke PL, Shih JH, Turkbey B, Wood BJ, Pinto PA: MRI-Targeted, Systematic, and Combined Biopsy for Prostate Cancer Diagnosis. *N Engl J Med.* Mar 5 2020; Vol.382(10) pp.917-928. PMCID:32130814
6. Masone MC: Can systematic biopsy be omitted from the prostate cancer diagnostic pathway? *Nature Reviews Urology.* Feb 2023; Vol.20(2) pp.65-65. <Go to ISI>://WOS:000912267900001. PMCID:WOS:000912267900001
7. Han M, Chang D, Kim C, Lee BJ, Zuo Y, Kim HJ, Petrisor D, Trock B, Partin AW, Rodriguez R, Carter HB, Allaf M, Kim J, Stoianovici D: Geometric evaluation of systematic transrectal ultrasound guided prostate biopsy. *J Urol.* Dec 2012; Vol.188(6) pp.2404-2409. PMCID:23088974
8. Bott SR, Young MP, Kellett MJ, Parkinson MC, Contributors to the UCLHTRPD: Anterior prostate cancer: is it more difficult to diagnose? *BJU Int.* Jun 2002; Vol.89(9) pp.886-889. https://www.ncbi.nlm.nih.gov/pubmed/12010233. PMCID:12010233
9. Kongnyuy M, Sidana A, George AK, Muthigi A, Iyer A, Fascelli M, Kadakia M, Frye TP, Ho R, Mertan F, Minhaj Siddiqui M, Su D, Merino MJ, Turkbey B, Choyke PL, Wood BJ, Pinto PA: The significance of anterior prostate lesions on multiparametric magnetic resonance imaging in African-American men. *Urol Oncol.* Jun 2016; Vol.34(6) pp.254 e215-221. https://www.ncbi.nlm.nih.gov/pubmed/26905304. PMCID:26905304
10. Lee AYM, Chen K, Tan YG, Lee HJ, Shutchaidat V, Fook-Chong S, Cheng CWS, Ho HSS, Yuen JSP, Ngo NT, Law YM, Tay KJ: Reducing the number of systematic biopsy cores in the era of MRI targeted biopsy-implications on clinically-significant prostate cancer detection and relevance to focal therapy planning. *Prostate Cancer Prostatic Dis.* Apr 2022; Vol.25(4) pp.720-726. https://www.ncbi.nlm.nih.gov/pubmed/35027690. PMCID:35027690
11. Drost FH, Osses D, Nieboer D, Bangma CH, Steyerberg EW, Roobol MJ, Schoots IG: Prostate Magnetic Resonance Imaging, with or Without Magnetic Resonance Imaging-targeted Biopsy, and Systematic Biopsy for Detecting Prostate Cancer: A Cochrane Systematic Review and Meta-analysis. *Eur Urol.* Jan 2020; Vol.77(1) pp.78-94. https://www.ncbi.nlm.nih.gov/pubmed/31326219. PMCID:31326219
12. Ahmed HU, Emberton M, Kepner G, Kepner J: A biomedical engineering approach to mitigate the errors of prostate biopsy. *Nature Reviews Urology.* 2012/04/01 2012; Vol.9(4) pp.227-231. https://doi.org/10.1038/nrurol.2012.3.

13. Gore JL, Shariat SF, Miles BJ, Kadmon D, Jiang N, Wheeler TM, Slawin KM: Optimal combinations of systematic sextant and laterally directed biopsies for the detection of prostate cancer. *J Urol.* May 2001; Vol.165(5) pp.1554-1559. PMCID:11342916
14. Kanao K, Eastham JA, Scardino PT, Reuter VE, Fine SW: Can transrectal needle biopsy be optimised to detect nearly all prostate cancer with a volume of ≥0.5 mL? A three-dimensional analysis. *BJU Int.* Nov 2013; Vol.112(7) pp.898-904. PMCID:23490279
15. Chang D, Chong X, Kim C, Jun C, Petrisor D, Han M, Stoianovici D: Geometric systematic prostate biopsy. *Minimally Invasive Therapy & Allied Technologies.* Nov 11 2016; pp.1-8. http://urobotics.urology.jhu.edu/pub/2016-chang-mitat.pdf PMCID:27760001
16. Stoianovici D, Chang D, Han M: Geometric Biopsy Plan Optimization. *USA Patent 10,751,034 B2* (C13488) Aug 25, 2020. https://urobotics.urology.jhu.edu/pub/2020-stoianovici-US10751034.pdf
17. Lim S, Jun C, Chang D, Petrisor D, Han M, Stoianovici D: Robotic Transrectal Ultrasound Guided Prostate Biopsy. *IEEE Trans Biomed Eng.* Sep 2019; Vol.66(9) pp.2527-2537. PMCID:30624210
18. Rezaee ME, Macura KJ, Trock B, Petrisor D, Burnett AL, Herati A, Pavlovich C, Han M, Stoianovici D: ABSTRACT#11: RANDOMIZED CONTROLLED TRIAL OF TRUS-ROBOT VS. URONAV BIOPSY IN THE DIAGNOSIS OF CLINICALLY SIGNIFICANT PROSTATE CANCER, PRELIMINARY RESULTS. *Engineering and Urology Society.* 4/30/2023 2023; Vol.36th Annual Meeting. https://urobotics.urology.jhu.edu/pub/2023-rezaee-EUS.pdf.
19. American College of Radiology: Prostate Imaging Reporting & Data System (PI-RADS Version 2.1). Available at: https://www.acr.org/-/media/ACR/Files/RADS/Pi-RADS/PIRADS-v2-1.pdf.
20. Epstein J, Walsh P, Carmichael M, Brendler C: Pathologic and clinical findings to predict tumor extent of nonpalpable (stage T1c) prostate cancer. *JAMA.* Feb 2 1994; Vol.271(5) pp.368-374.
21. STRICKER HJ, RUDDOCK LJ, WAN J, BELVILLE WD: Detection of Non-palpable Prostate Cancer. A Mathematical and Laboratory Model. *British Journal of Urology.* 1993; Vol.71(1) pp.43-46. https://bjui-journals.onlinelibrary.wiley.com/doi/abs/10.1111/j.1464-410X.1993.tb15878.x.
22. Coogan CL, Latchamsetty KC, Greenfield J, Corman JM, Lynch B, Porter CR: Increasing the number of biopsy cores improves the concordance of biopsy Gleason score to prostatectomy Gleason score. *BJU Int.* Aug 2005; Vol.96(3) pp.324-327. https://www.ncbi.nlm.nih.gov/pubmed/16042723. PMCID:16042723
23. Vashi AR, Wojno KJ, Gillespie B, Oesterling JE: A model for the number of cores per prostate biopsy based on patient age and prostate gland volume. *J Urol.* Mar 1998; Vol.159(3) pp.920-924. PMCID:9474183
24. Andriole GL: Pathology: the lottery of conventional prostate biopsy. *Nat Rev Urol.* Apr 2009; Vol.6(4) pp.188-189. https://www.ncbi.nlm.nih.gov/pubmed/19352393. PMCID:19352393
25. Bjurlin MA, Wysock JS, Taneja SS: Optimization of prostate biopsy: review of technique and complications. *Urol Clin North Am.* May 2014; Vol.41(2) pp.299-313. PMCID:24725491
26. de la Taille A, Antiphon P, Salomon L, Cherfan M, Porcher R, Hoznek A, Saint F, Vordos D, Cicco A, Yiou R, Zafrani ES, Chopin D, Abbou CC: Prospective evaluation of a 21-sample needle biopsy procedure designed to improve the prostate cancer detection rate. *Urology.* 2003/06/01/ 2003; Vol.61(6) pp.1181-1186. https://www.sciencedirect.com/science/article/pii/S0090429503001080.
27. Fleshner N, Klotz L: Role of "saturation biopsy" in the detection of prostate cancer among difficult diagnostic cases. *Urology.* 2002/07/01/ 2002; Vol.60(1) pp.93-97. https://www.sciencedirect.com/science/article/pii/S0090429502016254.
28. American Urological Association: Practicing Urologists in the United States. Available at: https://www.AUAnet.org/common/pdf/research/census/State-Urology-Workforce-Practice-US.pdf. Accessed June 2, 2023.
29. Rosenkrantz AB, Lepor H, Huang WC, Taneja SS: Practical Barriers to Obtaining Pre-Biopsy Prostate MRI: Assessment in Over 1,500 Consecutive Men Undergoing Prostate Biopsy in a Single Urologic Practice. *Urologia Internationalis.* 2016; Vol.97(2) pp.247-248. https://doi.org/10.1159/000446003.
30. Raman AG, Sarma KV, Raman SS, Priester AM, Mirak SA, Riskin-Jones HH, Dhinagar N, Speier W, Felker E, Sisk AE, Lu D, Kinnaird A, Reiter RE, Marks LS, Arnold CW: Optimizing Spatial Biopsy Sampling for

the Detection of Prostate Cancer. *J Urol.* Sep 2021; Vol.206(3) pp.595-603. https://www.ncbi.nlm.nih.gov/pubmed/33908801. PMCID:33908801

31. Panebianco V, Barchetti G, Simone G, Del Monte M, Ciardi A, Grompone MD, Campa R, Indino EL, Barchetti F, Sciarra A, Leonardo C, Gallucci M, Catalano C: Negative Multiparametric Magnetic Resonance Imaging for Prostate Cancer: What's Next? *Eur Urol.* Jul 2018; Vol.74(1) pp.48-54. https://www.ncbi.nlm.nih.gov/pubmed/29566957. PMCID:29566957
32. Baboudjian M, Uleri A, Beauval JB, Touzani A, Diamand R, Roche JB, Lacetera V, Lechevallier E, Roumeguere T, Simone G, Benamran D, Fourcade A, Fiard G, Peltier A, Ploussard G: MRI lesion size is more important than the number of positive biopsy cores in predicting adverse features and recurrence after radical prostatectomy: implications for active surveillance criteria in intermediate-risk patients. *Prostate Cancer and Prostatic Diseases.* Jul 14 2023. <Go to ISI>://WOS:001028412400001. PMCID:WOS:001028412400001
33. Cheng E, Davuluri M, Lewicki PJ, Hu JC, Basourakos SP: Developments in optimizing transperineal prostate biopsy. *Curr Opin Urol.* Jan 1 2022; Vol.32(1) pp.85-90. PMCID:34783715
34. Kepner G, Kepner J: Transperineal prostate biopsy: analysis of a uniform core sampling pattern that yields data on tumor volume limits in negative biopsies. *Theor Biol Med Model.* Jun 2010; Vol.17 pp.7-23.
35. Schweikard A, Schlaefer A, Adler JR, Jr.: Resampling: an optimization method for inverse planning in robotic radiosurgery. *Med Phys.* Nov 2006; Vol.33(11) pp.4005-4011. https://www.ncbi.nlm.nih.gov/pubmed/17153380. PMCID:17153380
36. Tanaka D, Shimada K, Rossi MR, Rabin Y: Towards intra-operative computerized planning of prostate cryosurgery. *Int J Med Robot.* Mar 2007; Vol.3 pp.10-19. https://www.ncbi.nlm.nih.gov/pubmed/17441020. PMCID:17441020
37. Kasivisvanathan V, Stabile A, Neves JB, Giganti F, Valerio M, Shanmugabavan Y, Clement KD, Sarkar D, Philippou Y, Thurtle D, Deeks J, Emberton M, Takwoingi Y, Moore CM: Magnetic Resonance Imaging-targeted Biopsy Versus Systematic Biopsy in the Detection of Prostate Cancer: A Systematic Review and Meta-analysis. *Eur Urol.* Sep 2019; Vol.76(3) pp.284-303. https://www.ncbi.nlm.nih.gov/pubmed/31130434. PMCID:31130434

SUPPLEMENT:

Capsule Based 3D Systematic Biopsy Optimization:

A biopsy plan defines the location of its component cores. SB plan optimization methods can be employed to maximize the likelihood of sampling csPCa (or csCDP) based on a patient's MRI and/or ultrasound images. Optimizing the plan for a patient, or personalizing the biopsy plan, is a complex task. A biopsy sample is not only defined by a core center point, but also by the direction of the core. The core direction follows that of the biopsy needle, which is constrained by the TRUS probe passing the anal sphincter. The planning and sampling problems are interrelated and so one cannot calculate a biopsy plan independently from the way that the biopsy is to be taken. However, the biopsy optimization may be estimated ahead of biopsy based on the MRI images.

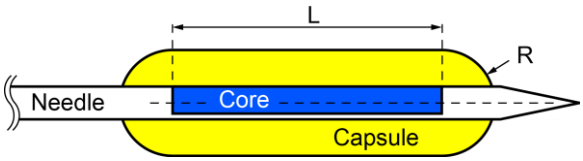

Figure 4: Capsule Model

We have developed a 3D geometric biopsy optimization method [15, 16], that was built upon the 2D approach of [34] and formulated to include the constraints of the actual biopsy sampling [17]. A "Capsule" model consists of a cylindrical shape with semispherical ends (yellow shape in Figure 4). The length L of the Capsule matches the length of the sample magazine of the biopsy needle, and its radius R matches the lowest radius of an assumed spherical tumor to be detected by the core. We have previously shown that if the center of a lesion is located within the Capsule, the biopsy samples the lesion [15]. We have also previously shown that CDP may be defined by the ration of the prostate volume within the Capsules relative to the total prostate gland volume [15], $CDP = \frac{V_p \cap (V_c^1 \cup V_c^2 \ldots \cup V_c^n)}{V_p}$, where V_p is the total prostate volume, n is the number of cores, $V_c^i, i = 1 \ldots n$ are the Capsule volumes, and symbols $\cap$ and $\cup$ are volume intersection and union, respectively. Since the fraction denominator V_p is always larger, then $CDP < 1$.

By size, csPCa is commonly considered that of volume ≥0.5cm^3 [20]. The shape of tumors is not spherical, however, considering the tumor spherical gives the lowest radial size [15] and so provides a worst case scenario for the CDP. The radius of a 0.5 cm^3 sphere is 4.924 mm, approximately 5mm. Therefore, with a capsule size R ≥ 5 mm, the CDP quantifies the likelihood of sampling csPCa. And so, the Capsule is the prostatic volume-unit with which a biopsy core samples the smallest csPCa.

As such, for a given biopsy plan the CDP equation provides a number giving the likelihood of sampling csPCa with that plan. Changing the plan may provide higher or lower CDP and so the plan may be optimized to maximize it. Our optimization [16] is an itterative pattern searching algorithm similar to so called sphere packing algorithms used in radio- and cryo-surgery planning [35, 36]. To increase CDP, the algorithm attempts to distribute the capsules so that they cover as much of the gland as possible, excluding the urethra. At combined TB and SB the optimization also accounts for the locations of the TB cores that are locked in position based on MRI findings. The CDP method applies to any biopsy plan, optimized or template based.

The software was written in C++ (Visual Studio, Microsoft Corp.) with open source Visualization Toolkit (VTK), Insight Toolkit (ITK), and Grassroots Digital Imaging and Communications in Medicine (DICOM) (GDCM) libraries.